Climate Dynamics (2019) 53:5101–5118
https://doi.org/10.1007/s00382-019-04852-8

Assessment of climatological tropical cyclone activity over the north Indian Ocean in the CORDEX-South Asia regional climate models

S. Vishnu[1,2] · J. Sanjay[1] · R. Krishnan[1]

Received: 18 March 2019 / Accepted: 10 June 2019 / Published online: 18 June 2019

Abstract
This study evaluates the ability of the regional climate models (RCMs) in the Coordinated Regional Climate Downscaling Experiment for South Asia (CORDEX-SA) to simulate the tropical cyclone activity in the north Indian Ocean. The RCMs used in the CORDEX-SA are Rossby Centre regional atmospheric model version 4 (RCA4) and Regional Climatic Model version 4 (RegCM4) forced by the ECMWF Interim Reanalysis (ERA-Interim) from 1989 to 2008. Both models have reasonable skill in capturing the observed climatological seasonal and spatial distribution of the genesis and track of the tropical cyclones. However, the two issues faced are (i) in RegCM4 model, higher number of tropical cyclones throughout the year compared to observations in addition to the unrealistic simulation of tropical cyclones during winter and (ii) in the RCA4 model, relatively higher tropical cyclone activity over the Arabian Sea compared to the Bay of Bengal. In the RCA4, the anomalous large-scale lower tropospheric cyclonic circulation observed over the southern Arabian Sea might be responsible for the overestimation in the number of tropical cyclones over there. In both models, the relationship between minimum pressure and the maximum wind is well simulated even though there is an underestimation in the intensity of the tropical cyclones. Quantitative analysis of large-scale environmental parameters that influence the tropical cyclone activity using an index called genesis potential index showed that in the RegCM4 model, the model simulates seasonal variation (enhancement/suppression) of environmental conditions fairly good as seen in the observation. However, the model has higher number of tropical cyclones in all the seasons, which is due to the enhanced large scale dynamical and thermodynamical parameters. The cold and wet bias in the middle troposphere causes the reduction in the mid-layer saturation deficit throughout the year, which in turn favours an unrealistic high number of tropical cyclone genesis. Therefore, the changes in the large scale dynamics and relatively saturated middle troposphere in the model might be responsible for the higher number of tropical cyclones.

Keywords CORDEX · Tropical cyclone · Indian Ocean · Regional climate model · Genesis potential index

1 Introduction

Tropical cyclones (TCs) are synoptic scale low-pressure systems formed in the tropical oceans having strong cyclonic winds with organized convection and heavy rainfall. It has devastating consequences with its destructive winds, torrential rains and storm surge causing considerable damage to life and property. A total of 150 TCs developed over the northern Indian Ocean (NIO) from 1981 through 2009, with majority of the TCs formed in the Bay of Bengal (BoB; Li et al. 2013) basin. The annual cycle of TCs in the BoB and Arabian Sea (AS) show prominent double peak occurring during the monsoon transition periods (April–May and October–December) whereas a single peak is dominant during the corresponding solar summer season in other ocean basins (Li et al. 2013). The bimodal nature in the occurrence of TCs over Indian Ocean may either due to the presence of monsoon trough over open ocean during pre-monsoon and post-monsoon seasons (Lee et al. 1989) or due to the presence of the strong vertical wind shear during the summer monsoon season which suppresses the cyclonic activity during the peak summer season (Gray 1968; DeMaria 1996).

The interannual variation of TCs in the NIO shows strong relation with Indo-Pacific coupled processes such as El-Nino Southern Oscillation (ENSO) and Indian Ocean Dipole

✉ S. Vishnu
vishnuedv@gmail.com

[1] Centre for Climate Change Research, Indian Institute of Tropical Meteorology, Pune 411008, India

[2] Department of Earth and Planetary Science, University of California, Berkeley 94720, USA

(Singh 2008; Girishkumar and Ravichandran 2012; Felton et al. 2013). On intraseasonal time scales, the genesis, and intensification of TCs over NIO are mainly influenced by Madden–Julian oscillation (MJO) with higher propensity for the formation of TCs during the active phase of MJO in the Indian Ocean basin (Liebmann et al. 1994; Goswami et al. 2003; Krishnamohan et al. 2012; Girishkumar et al. 2015 and reference therein).

Generally, TCs form over warm tropical oceans by taking energy (latent heat) from the underlying warmer ocean (Emanuel 2003). Hence, how TC activity changes under a warming climate is a fundamental question to understand. In a warming environment, the increase in greenhouse gas concentration increases the net surface radiative flux, which results in the intensification of TCs with a higher rate (Emanuel 2013). The intensification of TCs in the increase in greenhouse gas content is confirmed from the model experiments with General Circulation Models (GCM, Emanuel 1987; Bender et al. 2010). Even though the thermodynamic potential of TCs increases as the planet warms, the frequency of the TCs is determined by several factors which include environmental low-level vorticity, vertical wind shear, and middle layer humidity. The response of these factors in a warming environment may result in a reduction in the number of global TCs (Knutson et al. 2010).

Attempts to estimate the effect of global warming on TCs in a GCM started in the last decades of the twentieth century (Broccoli and Manabe 1990). However, the simulation of TCs by using numerical models has been a great challenge. GCM with low resolution (Vitart et al. 1997; Bengtsson et al. 2006) and medium resolution (Sugi et al. 2002; McDonald et al. 2005; Bengtsson et al. 2007) were used for the simulation and analysis of TCs. Even though these models failed to simulate the mesoscale features of TCs, they reproduced the observed climatology and interannual variability of TC reasonably well (Sugi et al. 2002; McDonald et al. 2005; Bengtsson et al. 2007). The inadequate simulation of TCs in the coarse resolution climate model is mainly due to the insufficient representation of the inner core structure of TC which arise from the large grid scale of the model compared to the typical size of TC (Vitart et al. 1997; McDonald et al. 2005). Hence, there is much demand for high-resolution climate models which can simulate the inner core structure of TC; however, it is computationally expensive.

An alternative method is to downscale the coarser resolution GCM output using statistical or dynamical methods. The dynamical downscaling is carried out by using a high-resolution regional climate model (RCM) over a specific region which can provide detailed information on TC activity (Camargo et al. 2007b; Knutson et al. 2007; Diro et al. 2014; Fuentes-Franco et al. 2017). Several previous studies have discussed the ability of RCMs in simulating the TCs reasonably good. Camargo et al. (2007b) showed that RCMs have the much-improved skill to reproduce the TC activity compared to its low resolution forcing. Knutson et al. (2007), showed that high-resolution RCM captures the decadal variability of TCs over the Atlantic Ocean and could reproduce its relationship with ENSO reasonably good compared to low-resolution models. In the Indian Ocean, Murakami et al. (2013) showed that high-resolution RCM has reasonable skill in reproducing the spatial variation of TC activity; however, the ability of the RCM depends on the forcing, parent GCM models. The capability of RCM to capture the TC activity is sensitive to the several factors such as resolution of the model (Fuentes-Franco et al. 2017), convective schemes (Diro et al. 2014; Fuentes-Franco et al. 2017), flux parameterization (Fuentes-Franco et al. 2017), and boundary forcing (Murakami et al. 2013; Diro et al. 2014).

In the past decades, several international projects have performed the dynamical downscaling of GCMs using RCMs for future climate projections (Fu et al. 2005; Christensen et al. 2007). Coordinated Regional Climate Downscaling Experiment (CORDEX; Giorgi et al. 2009) coordinated by the World Climate Research Programme (WCRP) regional activity has generated an ensemble of regional climate scenarios for South Asia by dynamical downscaling the outputs of several atmosphere–ocean global climate models (AOGCMs) that participated in the Coupled Model Intercomparison Project Phase 5 (CMIP5; Taylor et al. 2012) using multiple RCMs. The CORDEX South Asia (CORDEX-SA) RCM outputs are suitable to provide projections of TC activity over the NIO till the end of the twenty first century as these model domains cover most of the Indian Ocean basin with a reasonable fine-resolution (50 km) for simulating TCs. Although some previous studies attempted to evaluate precipitation and temperature simulated by these RCMs over South Asia (Choudhary et al. 2017; Singh et al. 2017; Sanjay et al. 2017), no attempts have been made to examine their ability to simulate TC activity over the NIO. This study intends to document the merits and demerits of the CORDEX RCMs in simulating the TC activity over NIO and their related large-scale environment. The knowledge of whether any systematic biases exist over the oceanic basin adjoining South Asia is vital in assessing the reliability of the downscaled future climate conditions simulated by these RCMs. This understanding is also useful to provide confidence when these RCM outputs are subsequently used in many climate impact studies over India and neighbouring countries within South Asia.

The focus of this study is to evaluate the ability of RCMs in the CORDEX-SA to simulate TC activity over NIO at spatial and temporal scales as compared to observations. Rest of the article organized as follows: Sect. 2 describes the data, models and methodology used in this study. Results obtained from the analysis are described in Sect. 3, including the climatology and intensity distribution of the simulated

TC activity, changes in the large-scale environment which is responsible for TC activities in the RCMs. Concluding and discussing the finding obtained from the analysis are in Sect. 4.

2 Data and methods

2.1 Data used

The information on genesis, track, and intensity of the observed TCs in the NIO are obtained from International Best Track Archive for Climate Stewardship (IBTrACS) for the period 1979–2008 (Knapp et al. 2010). Source of the TC data is selected as India Meteorology Department (IMD) since IMD is the regional specialized meteorological centre of World Meteorological Organization for NIO. The minimum central sea level pressure (MSLP) data for the TCs in the NIO are available only from 1990, so the analysis of the intensity of the TC is restricted to the period 1990–2008. The performance of the CORDEX RCMs for simulating the environmental factors influencing the TCs in the NIO is evaluated by comparing the simulated monthly mean upper-air fields, sea level pressure and sea surface temperature (SST) with the driving forcings provided from the European Centre for Medium Range Weather Forecasts (ECMWF) interim reanalyses of observations (ERA-Interim; Dee et al. 2011).

2.2 Models and experimental design

The results from the evaluation experiments conducted with two RCMs in the framework of the WCRP regional activity CORDEX (Giorgi et al. 2009) over the large domain (15.75°S–45.75°N; 19.25°–116.25°E) covering South Asia are presented in this study. These two RCMs, viz. Regional Climatic Model version 4 (RegCM4) and Rossby Centre regional atmospheric model version 4 (RCA4), describe the atmosphere and its coupling with the land surface with differing dynamics and physics formulations (see details in Table 1). The initial and six-hourly lateral boundary driving fields for these RCMs are provided from the ERA-interim reanalysis (Dee et al. 2011) interpolated onto a 1.5° by 1.5° horizontal grid. This reanalysis uses the SST obtained from the National Oceanic and Atmospheric Administration (NOAA) optimal interpolation (OI) weekly SST data (Reynolds et al. 2002). The model outputs are taken for 30 years from 1979 to 2008.

Table 1 The main characteristics of the CORDEX South Asia RCMs used in this study

CORDEX South Asia RCM	IITM-RegCM4	SMHI-RCA4
RCM description	The Abdus Salam International centre for Theoretical Physics (ICTP) Regional Climatic Model version 4 (RegCM4; Giorgi et al. 2012)	Rossby Centre regional atmospheric model version 4 (RCA4; Strandberg et al. 2015)
Contributing CORDEX modeling center	Centre for Climate Change Research (CCCR), Indian Institute of Tropical Meteorology (IITM), India	Rossby Centre, Swedish Meteorological and Hydrological Institute (SMHI), Sweden
Dynamics	Hydrostatic	Hydrostatic
Horizontal resolution	Rotated Mercator 50 km	Rotated pole 0.44° (~50 km)
Vertical levels	18 levels up to 50 hPa	24 levels up to 10 hPa
Parameterization of physical process		
Radiative transfer	Modified global model CCM3 scheme (Kiehl et al. 1996)	Modified numerical weather prediction model HIRLAM scheme (see Räisänen et al. (2000)
Cumulus convection	MIT scheme (Emanuel and Živkovic-Rothman 1999)	Bechtold-Kain-Fritsch deep and shallow convection schemes (Bechtold et al. 2001)
Resolved scale precipitation	Subgrid explicit moisture scheme (SUBEX; Pal et al. 2000)	Scheme of Rasch and Kristjánsson (1998)
Planetary boundary layer	UW turbulence closure model (Bretherton et al. 2004); a 1.5 order local, down-gradient diffusion scheme in which the velocity scale is based on turbulent kinetic energy (TKE)	Prognostic TKE scheme including moist processes in TKE calculation, combined with a diagnostic mixing length (see Lenderink and Holtslag 2004)
Land surface	Community Land Model version 4.5 (CLM4.5; Oleson et al. 2008)	A tiled land surface scheme (see Samuelsson et al. 2006)
Ocean fluxes	Zeng et al. (1998) scheme based on a Monin–Obukhov turbulence representation	

2.3 Tropical cyclone detection and tracking method

The TC detection method is similar to that reported in previous studies (Cha et al. 2011; Murakami et al. 2013; Jin et al. 2016). As the threshold of various variables depends on the model resolution, thresholds were modified to obtain an optimal match with the resolution of the models. The threshold of surface wind for the TCs is taken based on the study by Walsh et al. (2007), which describes the resolution dependence of TC detection algorithms in the climate models. As detection of TC highly linked to the detecting variables and threshold values, there might be uncertainty in the number of TCs among the algorithms and models. However, in this analysis, most of the detection variables incorporate from the previous study to remove the unsuitable candidates.

Further spatial and seasonal variation of TC using this detection method much matches with index (see Sect. 2.4) of TC using background conditions. The detection matrix is similar to the IMD criteria for TC detection, which uses minimum sea level pressure with closed contour criteria and surface wind speed criteria. All other detection variables are used to eliminate the non-tropical cyclone vortices such as extratropical cyclones, monsoon depression and other cyclonic vortices.

The detection criteria need to satisfy the following thresholds for various variables simulated by the RCMs:

(i) Location of the potential storm is a local minimum of sea level pressure with at least one closed contour with an interval of 2 hPa, which is estimated following Praveen et al. (2015). (ii) The maximum surface wind at 10 m exceeds the wind speed threshold of 17.5 ms^{-1} suggested by Walsh et al. (2007); this maximum wind threshold should be satisfied within 200 km of the potential storm centre to avoid false detection of weaker monsoon weather systems (Murakami et al. 2013). (iii) The deviations of tropospheric temperature (sum of temperature deviation at 200, 500, and 850 hPa levels) at the storm centre with respect to the environment should be positive. (iv) The local temperature anomaly at 200 hPa is higher than at 850 hPa. (v) The maximum wind speed at 850 hPa is higher than that at 200 hPa. (vi) The duration of storms is not shorter than 2 days.

The tracks are traced from these identified potential storms when at least 1 day of the storm satisfied the criteria (i)–(v) and criteria (i) for all the days. Detection of warm-core and the condition of wind speeds at lower troposphere be higher than upper-level wind speeds (criteria iii–v) are used to eliminate the extratropical cyclone (Krishnamurti et al. 1998; Sugi et al. 2002; Walsh et al. 2004). The location where an individual TC is first detected set as the genesis point. A TC genesis frequency (TGF) is defined by counting the number of TCs within a 2.5° × 2.5° longitude–latitude grid box over the NIO region. The daily location of potential storm counts binned into corresponding grid boxes for computing the TC frequency (TCF; also represents the track density) for each month in the NIO region.

2.4 Contributions of large-scale environmental processes to TC genesis

The influence of the large scale environmental factors on the genesis of TCs was quantitatively described by developing a genesis potential index (GPI; Emanuel and Nolan 2004; Emanuel 2010) and can be written as

$$GPI = Term1 \times Term2 \times Term3 \times Term4 \tag{1}$$

where $\text{Term}1 = |\eta|^3$, $\text{Term}2 = \left[max\left(V_{PI} - 35\right), 0\right]^2$, $\text{Term}3 = \chi^{\frac{-4}{3}}$, and $\text{Term}4 = \left(25 + V_{sh}\right)^{-4}$, η is the absolute vorticity at 850 hPa, V_{PI} is the maximum tropical cyclone potential intensity (PI) defined by Emanuel (1999). V_{sh} is the magnitude of the horizontal wind shear between 850 and 200 hPa. The parameter χ is defined as

$$\chi = \frac{\left(h^* - h_m\right)}{\left(h_o^* - h^*\right)} \tag{2}$$

where h^* is the saturation moist static energy of the free troposphere, h_m is the actual moist static energy of the middle troposphere (pressure-weighted mean over the layers 700–600 hPa), and h_o^* is the saturation moist static energy of the sea surface. This ratio gives a measure of the saturation deficit in the middle troposphere that must be eliminated by moist convective processes to the strength of the thermodynamic disequilibrium at the surface on which the fluxes fueling the convection depend. The nondimensional parameter χ is a measure of the moist saturation deficit of the middle troposphere, becomes higher as the middle troposphere dries. Emanuel (2010) showed that this TC genesis potential index captures those climate influences that act on small regional scales.

Li et al. (2013) modified the GPI equation to reveal the relative roles of large-scale environmental factors to the total changes in the GPI as

$$\delta\text{GPI} = \alpha 1 \times \delta\text{Term}1 + \alpha 2 \times \delta\text{Term}2 + \alpha 3 \times \delta\text{Term}3 + \alpha 4 \times \delta\text{Term}4 \tag{3}$$

The terms $\alpha 1$, $\alpha 2$, $\alpha 3$, and $\alpha 4$ are defined as

$$\alpha 1 = \overline{Term2 \times Term3 \times Term4},$$

$$\alpha 2 = \overline{Term1 \times Term3 \times Term4},$$

$$\alpha 3 = \overline{Term1 \times Term2 \times Term4},$$

$$\alpha 4 = \overline{Term1 \times Term2 \times Term3}$$

and

$$\delta GPI = GPI - \overline{GPI}.$$

Here, the bar indicates the mean state (climatology) and δ represents the perturbation of variables. We use a similar method to diagnose the difference in the CORDEX RCM in simulating the TC climatology over NIO, specifically for identifying the relative contributions of the four large-scale environmental processes represented by each term on the right-hand side of Eq. 3, viz. low level vorticity (Term1), potential intensity (Term2), mid-tropospheric moist saturation deficit (Term3), and vertical wind shear (Term4). In the case of the monthly evolution of TC, the bar indicates the annual mean and δ represents the monthly anomaly from the yearly mean. In the case of model bias, the bar represents the observation and δ describes the model difference from the observation.

3 Results

3.1 Tropical cyclone activity in models

3.1.1 Genesis

The 30 years (1979–2008) mean climatology of TGF (TC genesis density) from IBTrACS best track data, and the two CORDEX RCMs binned into 2.5 × 2.5 grid points over NIO are shown in Fig. 1 (left panel). The observed spatial distribution of TGF exhibits maximum density over two locations, viz, the BoB (primary) and the AS (secondary). Both CORDEX RCMs capture the two observed spatial peaks in TGF over NIO reasonably well, albeit better skill in the RegCM4 model (spatial correlation, r = 0.49) compared to the RCA4 model (r = 0.39). The relatively higher number of TC genesis over AS compared to BoB in the RCA4 model has resulted in the lower skill of the model to capture the observed spatial variability of TGF over NIO. Similar issue has been reported in some of the climate models (Murakami et al. 2013). Even though the RegCM4 model captures the

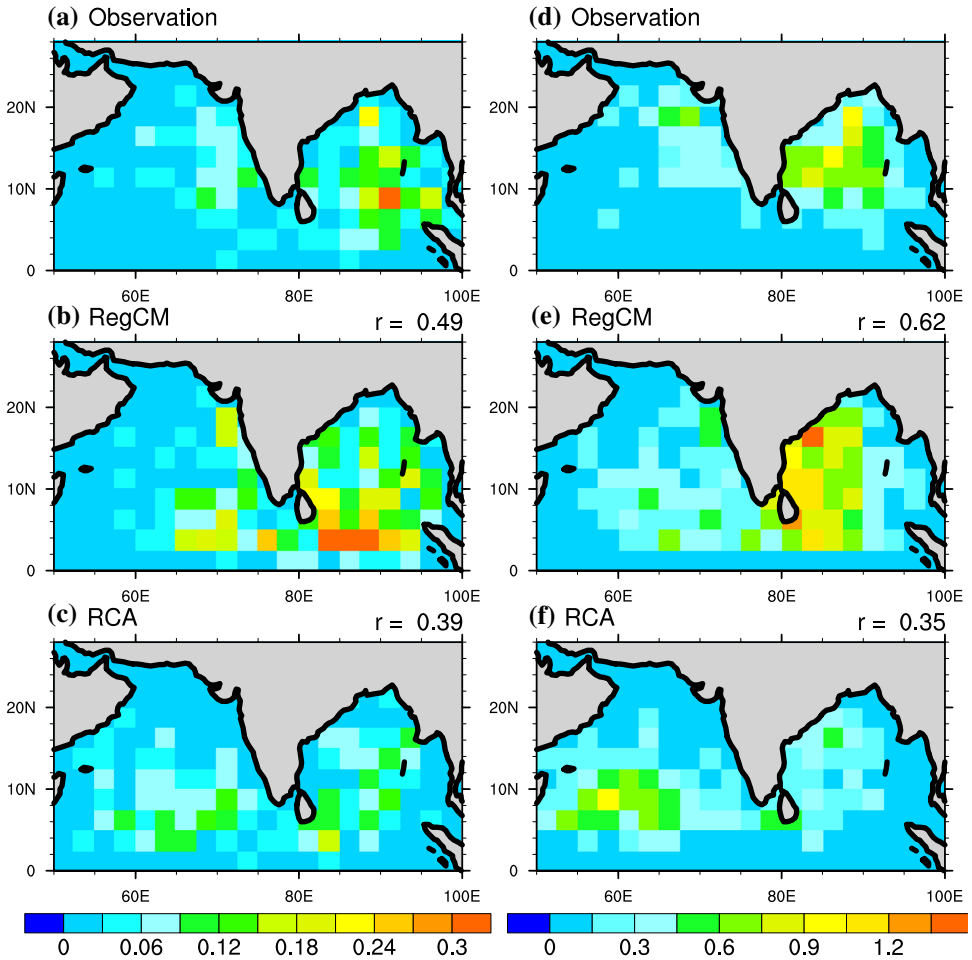

Fig. 1 Climatological annual mean tropical cyclone genesis frequency (TGF) from the **a** observations, and CORDEX regional models, **b** RegCM4 and **c** RCA4. **d**–**f** is the same as **a**–**c** but for tropical cyclone frequency (TCF; also represents TC track density). Climatology calculated from 1979 to 2008

spatial distribution of TGF, the annual frequency of TGF is higher in the RegCM4 (9 year^{-1}) compared to the observation (5 year^{-1}).

3.1.2 Tracks

The observed TCF (also represents TC track density) computed by binning daily TC positions into corresponding grid boxes also follow the spatial pattern of TGF concentrated in the NIO with two local maxima at locations closer to that of TGF (Fig. 1, right panels). The simulated TCF by CORDEX RCMs is comparable to the observations. The RegCM4 model has better skill to simulate the observed TC track with a spatial correlation coefficient of 0.62 compared to the RCA4 model (r = 0.35). In response to the higher number of TGF (Fig. 1), the RegCM4 model has higher TCF over NIO (both the AS and BoB basins). The relatively weaker skill of RCA4 model to simulate the spatial distribution of TCF is mainly due to the overestimation of TGF over AS and unrealistic westward propagation of TCs from the TC genesis location over southern AS (Fig. 1).

3.1.3 Intensity

The frequency distributions of the TC lifetime maximum surface velocity (MVEL) over NIO and MSLP simulated by the CORDEX RCMs having 50-km horizontal resolution are compared with the best-track data. This analysis will assess the dependency of the simulated TC intensity on the different representations for the dynamical and physical processes adopted in the RegCM4 and RCA4 models. Figure 2 shows that in the observation, frequency of occurrence of MVEL (Fig. 2a) and MSLP (Fig. 2b) distributed uniformly. However, the simulated TCs without sufficient horizontal resolution in the RCMs to resolve intense TCs, are skewed towards weak MVEL and high MSLP. The maximum MVEL simulated in RegCM4 (RCA4) model is 37.30 ms^{-1} (39.59 ms^{-1}). Hence, these models tend to overestimate the TCs of moderate intensity (MVEL ranging from 22 to 37 ms^{-1}) and do not capture single TC having MVEL values higher than 40 ms^{-1}.

The frequency distribution of MSLP simulated by the RCMs showed that the distributions simulated by RegCM4 and RCA4 models are too narrow and skewed towards higher MSLP above 990 hPa (Fig. 2b). Both RCMs tend to overestimate (underestimate) the MSLP above (below) 990 hPa. It appears that there is no significant difference in the MSLP distribution simulated by two RCMs. Further, the value of maximum MSLP of the strongest cyclone simulated by RegCM4 and RCA4 models are 979 hPa and 976 hPa, respectively. The overestimation (underestimation) in the number of weaker (stronger) TCs in the model might be due to the lack of sufficient spatial resolution to resolve intense

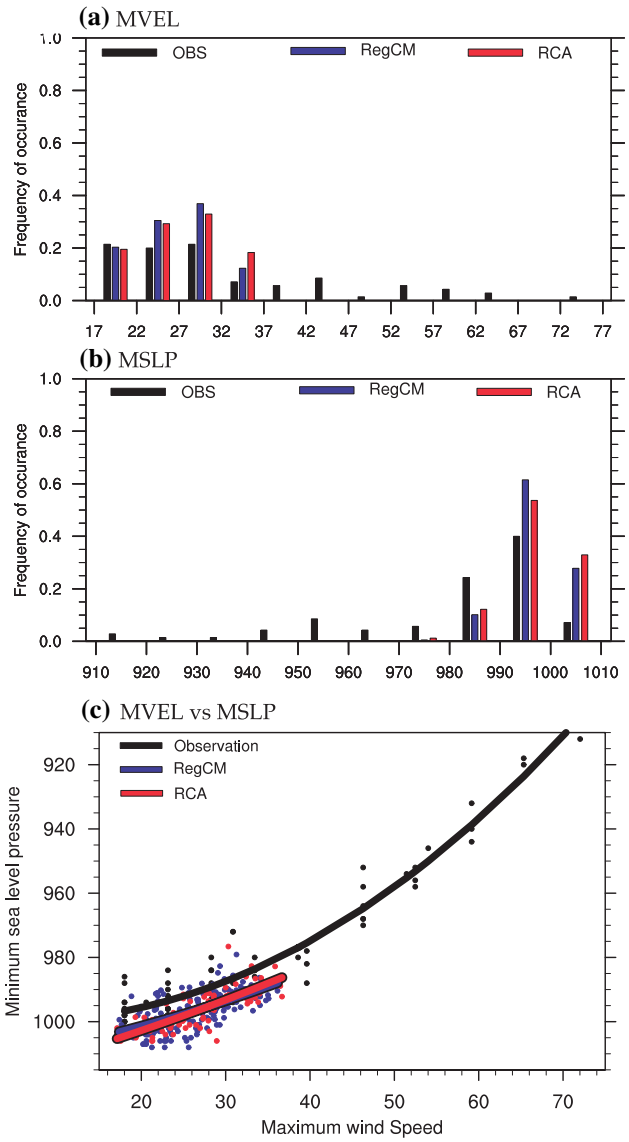

Fig. 2 Distribution of the TC lifetime **a** maximum wind speed (MVEL) and **b** minimum sea level pressure (MSLP) in the observed best-track data (black), CORDEX RegCM4 (blue) and RCA4 (red) RCM simulations for the period 1990–2008. **c** Scatter diagram of MVEL versus MSLP for these datasets, with solid curves showing the polynomial fit to the observed and model-simulated data points

TCs which has been reported in previous studies for other models (Murakami and Sugi 2010; Kim et al. 2014).

Figure 2c shows the scatter diagram of MVEL versus MSLP in observation and RCMs together with the lines denoting the second-order polynomial fit to the data points. Both the models simulate the observed relationship between MVEL and MSLP reasonably, although the magnitude of MSLP shows a positive bias for a given MVEL compared to the observation. This positive bias in the MSLP arises from the usage of instant MSLP in the model instead of minimum MSLP as used in the observation.

3.1.4 Annual cycle

The monthly variation in the number of TCs (with a standard error) over the NIO by the CORDEX RCMs is compared with the best-track data and is given in Fig. 3. The observed annual cycle of TC activity displays a bimodal nature having two peaks during the monsoon transition months (April–May and October–December), as reported by previous studies (e.g., Li et al. 2013). The CORDEX RCMs reasonably reproduces the observed double peak in the number of TCs, albeit higher values during the post-monsoon season. The observed occurrence of lesser genesis frequency of TC during the summer monsoon season (June–September), which is attributed to the presence of strong vertical wind shear during this season (e.g., Evan and Camargo 2011; Yanase et al. 2012) is simulated well by the two RCMs. However, the RegCM4 model overestimates the number of TC genesis for almost all the months. It may also be noted that the RegCM4 model simulated a remarkable amount of TC genesis during the winter season (January–March). This unrealistic higher number of TCs might be due to the occurrence of the higher fraction of TC genesis locations equatorward of NIO (see Fig. 1). In order to check this, monthly variation in the number of TCs after excluding the region below 5°N was also analyzed. It shows better seasonal variation in the number of TCs compared with the observation and specifically, the reduction in the unrealistic higher number of TCs during winter months in the RegCM model. Though the presence of the higher number of TC in the RegCM model still exists. Therefore overestimation in the number of TCs in the RegCM is not only from the near equator region.

3.2 Seasonal variability of TC and its related large scale environment

It is well known that no TC develops over the BoB (Li et al. 2013) and AS (Evan and Camargo 2011) during the primary summer monsoon months (July–August) when the southwest monsoon circulation dominates the large-scale features of the NIO basins with the monsoon trough at its most northerly position and located over the Indian subcontinent. The seasonal evolution of large-scale features explored in past studies (e.g., Gray 1968; Evan and Camargo 2011; Li et al. 2013) describes the environmental conditions relevant to TC genesis and intensification in NIO basins, viz SST, upper- and lower-level convergence, wind speed and direction, vertical wind shear, and low-level vorticity. These environmental parameters are analysed and compared with the CORDEX RCM outputs to understand their relative contribution to the discrepancies in the simulated cyclone activity over NIO.

Mean pattern of SST and surface wind in the observation and models are analysed separately for all the seasons (Figure not shown). The spatial pattern of SST in the observation shows relative cooling over the western Arabian Sea, which is mainly due to the wind-driven cooling over the western Arabian Sea region. It is observed that genesis of TCs mostly occur over the region where SST is higher than 26.5 °C, an empirical threshold value for the genesis of TC (Gray 1968). In the models, most of the TC genesis occurs over BoB and eastern part of the AS, as seen in the observation. It worth to note that simulation of TC genesis only occurs when the SST crosses the threshold. The model simulated surface wind is also similar to surface level circulation in the observation (Figure not shown).

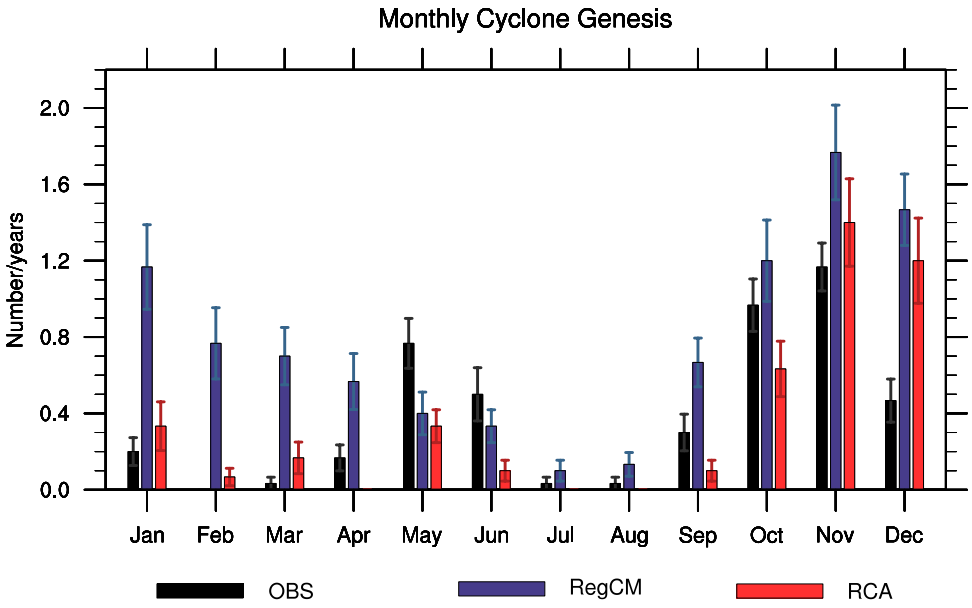

Fig. 3 Climatology of the monthly mean number of tropical cyclone genesis (bar) and its standard error (vertical line) over the NIO region based on observations (black), CORDEX regional models, RegCM4 (blue) and RCA4 (red). Climatology calculated from 1979 to 2008

The lower tropospheric level (850 hPa) realtive vorticity and wind over NIO simulated by two RCMs are shown in Fig. 4 along with observations. Observation shows that the genesis of TC occurs mostly over the region where there is background cyclonic vorticity field. Both RCMs capture the observed spatial pattern of lower level circulation and associated vorticity field. Even though RegCM4 simulate the observed circulation pattern, there is a southward shift in the mean vorticity field and circulation. Nevertheless, the region of TC genesis coincides with the positive vorticity values in the RegCM4 model. It may also be noted that even though the RegCM4 model simulates the positive vorticity field similar to the observation, it overestimates the number of the genesis of TC over the near-equatorial region during the winter season. The significant difference in the RCA4 model from the observation is the anomalous cyclonic circulation in the southern AS especially during pre-monsoon and post-monsoon season. Relatively higher values of positive vorticity over this region might be responsible for the higher number of TC genesis over the AS compared to the BoB in the RCA4 model.

Since vertical wind shear is an important factor that controls the genesis and intensification of TCs, vertical wind shear along with upper tropospheric level (200 hPa) wind in the models are compared with the observation and shown in Fig. 5. The genesis of TC occurs mainly over the region with less vertical wind shear except during the summer monsoon season (Fig. 5). It is evident that the weakening of wind shear over the southern part of north India except summer monsoon season can result in more number of TC genesis in the models. It may be noted that the westerly anomalies in the lower troposphere (Fig. 4) along with the unchanged westerly wind in the upper troposphere (Fig. 5) might be responsible for the weakening of wind shear. The unrealistic weakening of wind shear towards the equator in the NIO (AS and BoB) during the winter season in the RegCM4 model could be responsible for the simulation of higher number of TCs. Hence, misrepresentation of the atmospheric dynamics has a significant role in the unrealistic simulation of TCs in the models.

Since the large-scale parameters discussed above are not a comprehensive list of environmental conditions which are essential for the genesis and intensification of TC, we next analysed a quantitative method that including most of the large-scale dynamical and thermodynamical variables that influence the genesis and intensification of TC by using an empirical index called GPI. This analysis was restricted to the RegCM4 model because some of the variables required for the GPI in the RCA4 model is not readily available.

3.3 Model simulated large scale environment for the TC activity using GPI

GPI has been used as a tool to analyze the intra-seasonal, seasonal and inter-annual variation of TC activity in various tropical ocean basins (Camargo et al. 2007a, 2009) including

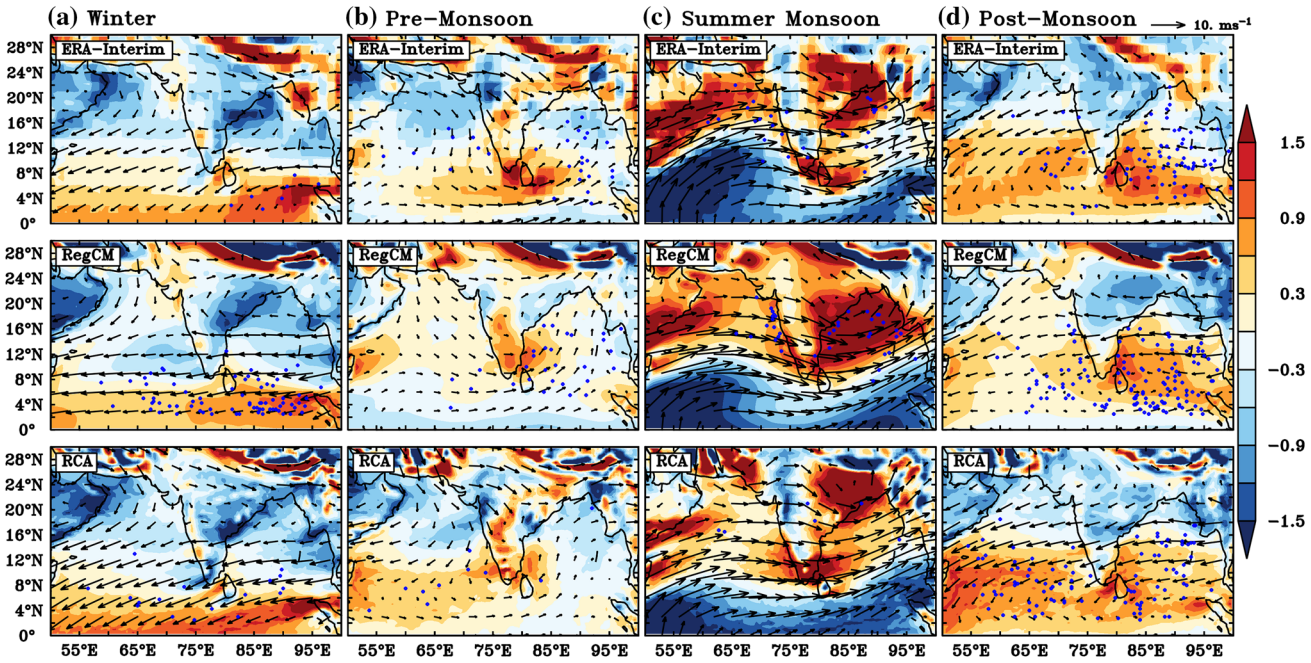

Fig. 4 Maps of seasonal mean low-level (850 hPa) relative vorticity (shaded) and wind (vector) during the **a** winter (January–March), **b** pre-monsoon (April–May), **c** summer monsoon (June–September) and **d** post-monsoon (October–December) season. Blue dots denote TC genesis locations for each season. The period for vorticity, winds, and cyclogenesis is 1979–2008. The first row represents the observation, second and third for RegCM4 and RCA4 respectively

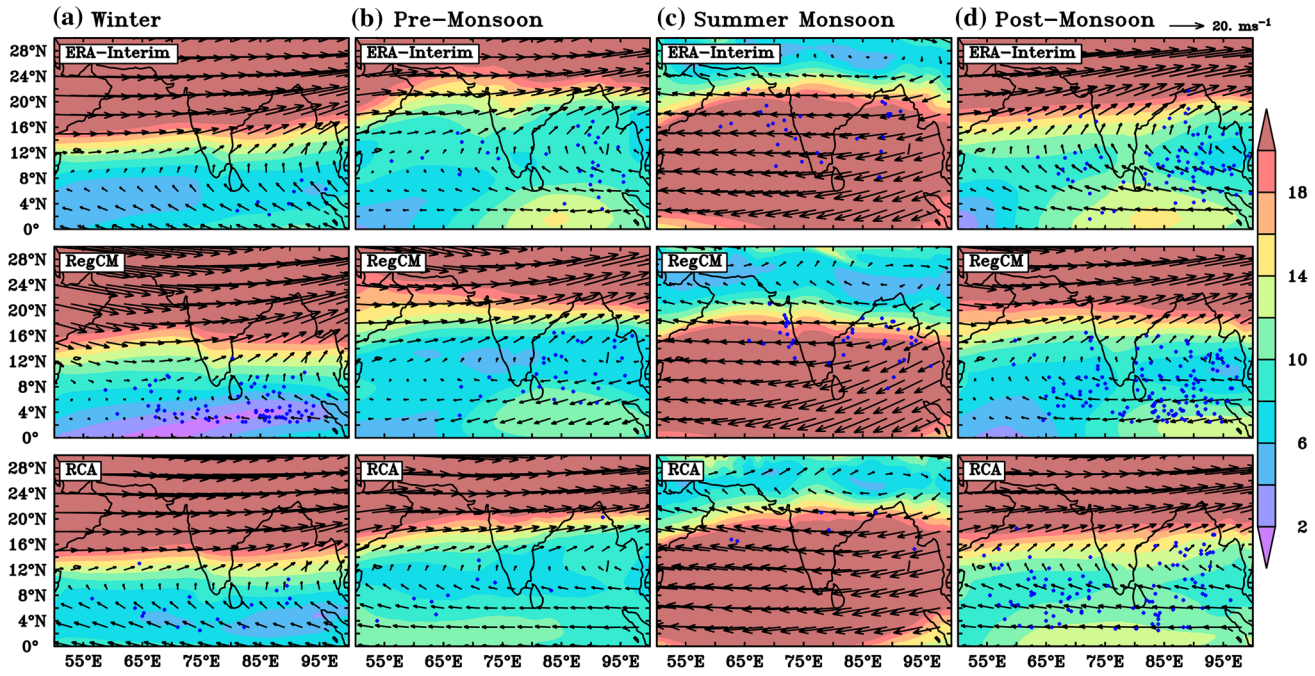

Fig. 5 Same as Fig. 4 but for vertical wind shear (shaded) and winds (vector) at 200 hPa

Indian Ocean (Yanase et al. 2012; Li et al. 2013; Girishkumar et al. 2015) in observation and models in various possible aspects (McDonald et al. 2005; Camargo et al. 2007b, c).

3.3.1 Climatological seasonal variations

The relative contribution of various large-scale environmental factors causing the bimodal nature in the seasonal cycle of TC genesis over the BoB (5°–15°N, 80°–95°E) and AS (5°–15°N, 65°–75°E) is investigated using the δGPI method (Eq. 3). This analysis is similar to the analysis by Li et al. (2013) to investigate the role of environmental conditions in the seasonal variation of TC activity in the model. Figure 6 shows the monthly changes in the GPI and contributions from each term (right-hand side of Eq. (3)) in the GPI equation to the change in GPI-(left-hand side of Eq. (3)) diagnosed using the ERA-Interim reanalysis based on observations (Fig. 6a, b) and using the RegCM4 model outputs (Fig. 6c, d). It is evident that the observed minimum in δGPI over both BoB and AS basins during the boreal winter months (January–March) are mainly attributed to the environmental lower tropospheric vorticity (Term1), potential intensity (Term2; mainly due to the sea surface cooling in the winter season), and moisture saturation deficit (Term3). The favourable condition of these large scale environmental factors along with the weaker wind shear (Term4) results in observed maxima in δGPI during the monsoon transition months (April–May and October–December) over both of the NIO basins. The minimum in δGPI during the summer monsoon season (June–September) over the BoB is primarily due to environmental vertical shear, although the moisture saturation deficit tends to enhance GPI in this season. The δGPI minima over the AS basin during the monsoon season has an additional contribution from the lower tropospheric vorticity.

The RegCM4 simulation captures the observed bimodal characteristic in the seasonal cycle of TC genesis reasonably well in the both the NIO basins (BoB and AS), despite overestimation of δGPI in all months (Fig. 6c, d). This issue could be attributed to the overestimation of the individual large-scale factors influencing the changes in δGPI in the model. It may also be noted that relatively higher GPI values over BoB during summer monsoon season might indicate the genesis of the higher number of monsoon depression (weaker systems compared to TC; see Vishnu et al. 2016) in the model. The relatively larger δGPI in the summer monsoon season is due to the combined effect of reduction in the saturation deficit (increase in the moisture availability in the middle troposphere) and favourable lower tropospheric vorticity which overcomes the unfavourable environmental vertical shear and the potential intensity for the genesis of the TC.

The dominant environmental factors responsible for the seasonal evolution of TC over BoB and AS in the observation and model are diagnosed by calculating the seasonal difference in each large-scale environmental variables using GPI equation (Eq. 3) and are depicted in Table 2. In the observation, the the cyclonic activity increases from winter

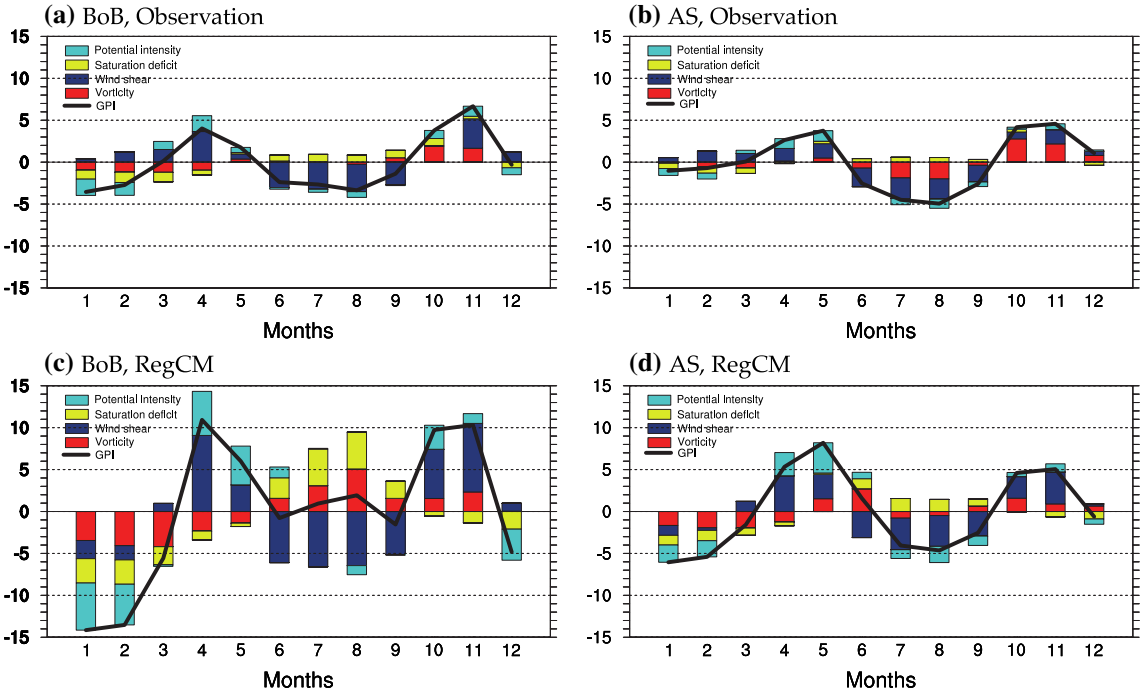

Fig. 6 Climatology monthly mean variation of GPI (line) and relative contribution of each environmental terms such as potential intensity, saturation deficit, wind shear and low-level absolute vorticity, to the changes in the GPI over **a** Bay of Bengal (5°–15°N, 80°–95°E) and **b** Arabian Sea (5°–15°N, 65°–75°E) in the observation. **c**, **d** are the same as **a**, **b** but for the model

Table 2 Contributions of each terms to the GPI in the Bay of Bengal and Arabian Sea during the increasing and decreasing formation periods

	δGPI	δVorticity	δWind shear	δSaturation deficit	δPotential intensity
Bay of Bengal					
Observation					
JFM-AM	4.94	0.82 (17)	1.08 (22)	0.95 (19)	2.09 (42)*
AM-JJAS	−5.33	0.41 (−8)	−5.18 (97)*	1.03 (−19)	−1.59 (30)
JJAS-OND	5.83	1.07 (18)	4.66 (80)*	−0.68 (−11)	0.78 (13)
OND-JFM	−5.43	−2.30 (42)*	−0.55 (10)	−1.30 (24)	−1.28 (24)
Model					
JFM-AM	19.54	2.04 (10)	7.09 (36)	1.92 (10)	8.49 (44)*
AM-JJAS	−8.33	4.70 (−56)	−12.20 (146)*	4.05 (−49)	−4.87 (59)
JJAS-OND	4.93	−1.52 (−31)	11.07 (225)*	−4.66 (−95)	0.04 (1)
OND-JFM	−16.14	−5.22 (32)	−5.96 (37)*	−1.31 (8)	−3.65 (23)
Arabian Sea					
Observation					
JFM-AM	3.75	0.79 (21)	0.64 (17)	0.73 (20)	1.59 (42)*
AM-JJAS	−6.83	−1.56 (23)	−3.87 (57)*	0.41 (−6)	−1.81 (26)
JJAS-OND	6.92	3.16 (46)	3.26 (47)*	−0.47 (−7)	0.97 (14)
OND-JFM	−3.83	−2.39 (62)*	−0.03 (1)	−0.66 (17)	−0.75 (20)
Model					
JFM-AM	11.10	1.99 (18)	3.68 (33)	0.94 (8)	4.49 (41)*
AM-JJAS	−9.19	0.40 (−4)	−6.96 (75)*	1.39 (−15)	−4.02 (44)
JJAS-OND	5.44	0.52 (10)	5.59 (103)*	−1.78 (−33)	1.11 (20)
OND-JFM	−7.36	−2.91 (40)*	−2.31 (31)	−0.56 (8)	−1.58 (21)

Percentage contribution is shown in brackets. Periods are winter (January–March; JFM), pre-monsoon (April–May; AM), summer monsoon (June–September; JJAS), post monsoon (October–December; OND). The dominant term is labeled with an asterisk

season to pre-monsoon season (see Figs. 3 and 6) mainly due to the enhanced potential intensity (42% in BoB and AS), which may be due to the relative higher SST in the pre-monsoon season compared to the winter season in the NIO. All the other factors also favour the increase in the TC activity over the BoB and AS in the pre-monsoon season compared to the winter season. The second increase in the TC occurs in the post-monsoon season to the summer monsoon season. This increase is mainly due to the decrease in the wind shear (80% in the BoB and 103% in the AS) in both the basins. In addition to the weakening of environmental wind shear, the enhanced lower tropospheric vorticity, and potential intensity overcome the increase in the moisture saturation deficit (Table 2) and hence favours the TC genesis. The withdrawal of summer monsoon and associated weakening of monsoon circulation may be responsible for the decrease in the wind shear and an increase in the moisture saturation deficit. It is seen that the environmental changes during the two peak TC seasons are different. While all the environmental factors are favourable during the pre-monsoon season, environmental factors except saturation deficit are favourable in the post-monsoon season.

The first decrease in the genesis of TC occurs in summer monsoon season compared to the pre-monsoon season (see Figs. 3 and 6) in both the basins. The dominant factor for this decrease in the TC is the increase in the wind shear (primary contribution; 97% in BoB and 57% in the AS) (Table 2). In addition to the increase in the wind shear, decrease in the potential intensity (30%) in the BoB and reduction in the potential intensity (26%) and lower tropospheric vorticity (23%) in the AS overwhelmed the decrease in the moisture saturation deficit (− 19% in BoB and − 6% in AS), hence tends the suppression of TC. This complex combination of all the environmental factors lowers TC activity in the NIO during summer monsoon season, rather than the enhanced wind shear alone as pointed out by Gray (1968). This has already reported by Li et al. (2013). The second decrease in the TC activity is during the winter season compared to the post-monsoon season. All the large-scale environmental factors are unfavourable for the TC activity during the winter season with the dominant contribution from the decrease in the background lower tropospheric vorticity (42% in BoB and 62% in AS).

The RegCM4 model captures well the difference in the background environmental variables in the different seasons, as seen in the observation (Table 2). The model capability of the model to simulate the seasonal changes in the environmental conditions, which is necessary for the genesis of TC, leads to the model efficiency to simulate the seasonal variations in the TC activities. However, the model simulation shows some difference from the observation. There is a substantial rate of enhanced environmental lower tropospheric vorticity in the BoB and AS during the summer monsoon to the pre-monsoon season in the model compared to observation. This anomalous enhancement of lower tropospheric vorticity is responsible for the higher value of GPI during the summer monsoon in the model (Fig. 6). It may also be noted that the decrease in the environmental lower tropospheric vorticity during the post-monsoon season over the BoB compared to the summer monsoon season in the model is opposite to the observation. During the winter season, the dominant factor responsible for the decrease in the TC over BoB is the increase in the wind shear in the model rather than the reduction in the low tropospheric environmental vorticity as observed. The differences in the model simulation may arise from the differences in the circulation and thermodynamic parameters. Hence, in the next section, the differences in the model simulated TCs from the observation in various seasons, and the environmental factors responsible for these differences are analyzed using the GPI.

3.3.2 Model differences

The discrepancies in the model simulation of TCs over NIO during various seasons and the reasons for this are investigated using GPI and is depicted in Fig. 7. The difference in the simulated GPI from observed GPI was calculated using Eqs. (1) and (3) (second and third row of Fig. 7), and it shows that estimation calculated using both equations are same. Hence it gives the confidence to computing the relative contribution each variable on the difference in GPI in the model using Eq. (3). The RegCM4 model simulates higher number of TCs during all seasons and therefore have greater GPI, and it is evident that the related terms of GPI enhance favourable environmental condition for the genesis of the TC (Fig. 7).

In the winter season, the region of enhanced TC activity is near to the equator (Fig. 7a). More favourable environmental conditions for the TC genesis near to the equator is seen from the enhanced GPI. The reduction in the wind shear and saturation deficit are mainly responsible for this unrealistically high TC activity during the winter season (Fig. 7a). The decline in the vertical wind shear over the near-equatorial region during the winter season is mainly due to the weakening of wind in the lower and upper troposphere. It is seen that weakening of northwesterly (southeasterly) by an unrealistic anomalous southeasterly (northwesterly) in the lower (upper) troposphere is responsible for the weakening of wind in the model (second row of Fig. 8a). The reduction in the saturation deficit is due to the enhanced specific humidity and decreased air temperature over the middle tropospheric level (700–600 hPa; the third row of Fig. 8a). Increased moisture content and decreased temperature in a developing system can quickly saturate the middle tropospheric levels (Emanuel 2010, 2013), which in

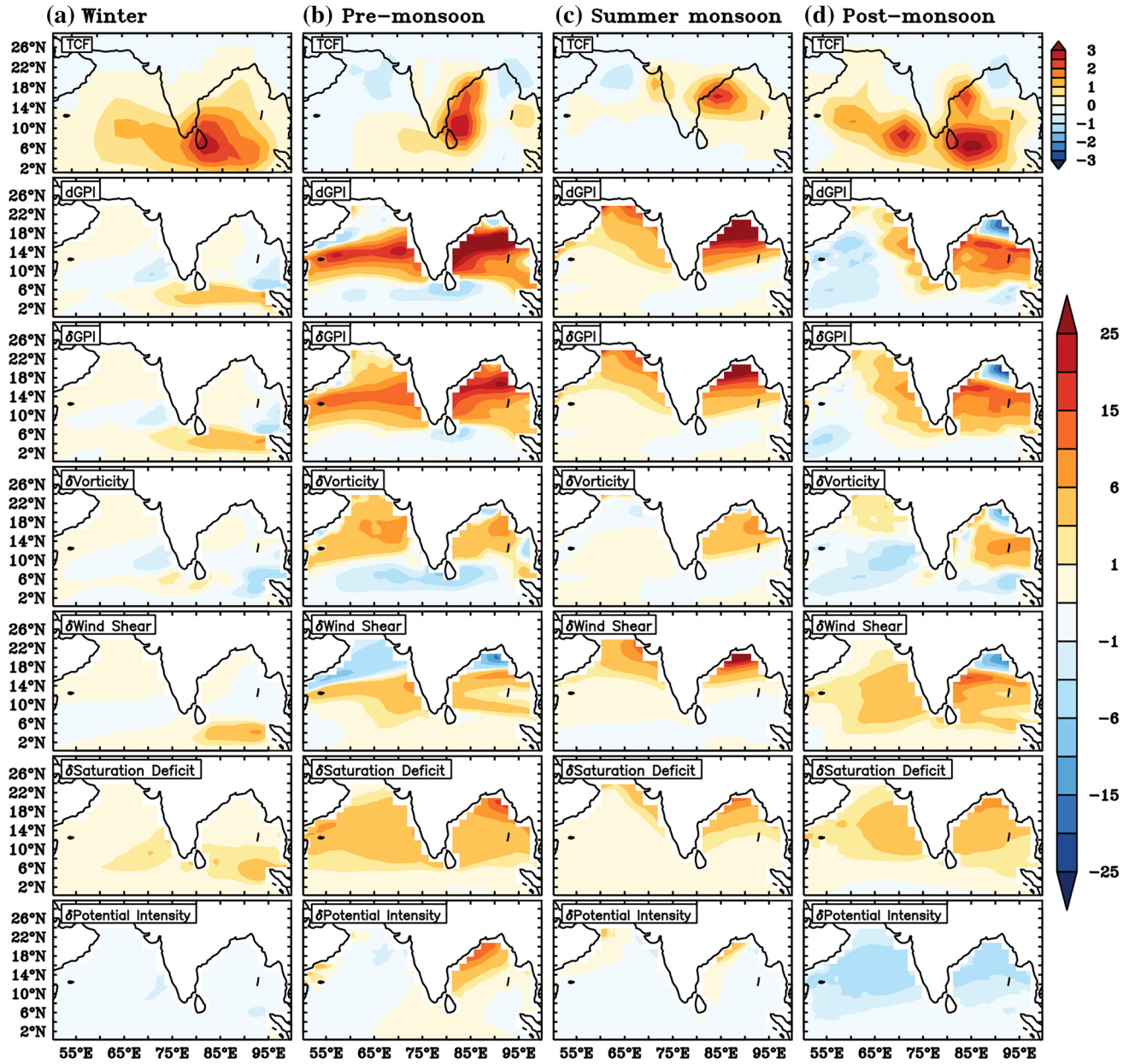

Fig. 7 Model bias in the tropical cyclone frequency (TCF; first row), the GPI (second row) calculated using Eq. (1), GPI (third row) derived from Eq. (3) and each term in the GPI equation such as environmental vorticity (fourth row), wind shear (fifth row), saturation deficit (sixth row) and potential intensity (seventh row) during the **a** winter, **b** pre-monsoon, **c** summer monsoon and **d** post-monsoon season

turn significantly reduces the saturation deficit in the middle layer leading to favourable condition for the TC genesis/intensification.

In the pre-monsoon season, the RegCM4 model has more TCF over western BoB compared to the observation (Fig. 7b). The GPI analysis shows that higher GPI over NIO is due to the more favourable condition of all the environmental variables in the model compared to the observation (Fig. 7b). Anomalous easterly wind in the lower tropospheric level reduces the mean westerly wind over the BoB, and it causes anomalous cyclonic vorticity over there (first row of Fig. 8b). The reduction in wind shear is mainly due to the decrease in the wind speed in the upper troposphere (second row of Fig. 8b). As in the winter season, the increasing specific humidity in a decreasing temperature reduces the saturation deficit in the model (third row of Fig. 8b). The relative dryness of the boundary layer simulated in the model over the SST background which is consistent with observation (model and observed SST are from ERA-Interim as the model SST updated from the ERA-Interim) is responsible

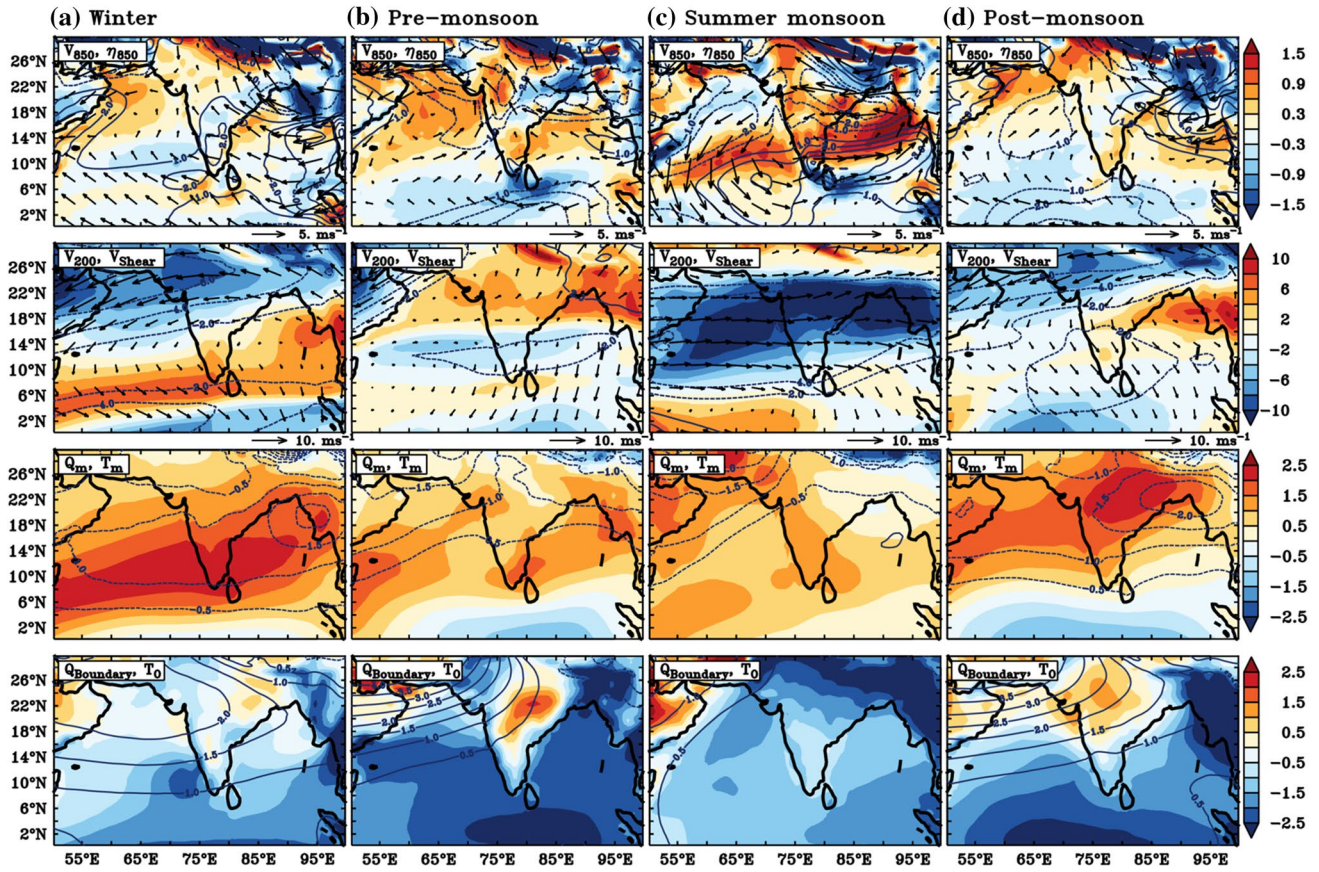

Fig. 8 Model biases in the various meteorological parameters compared to the observation during the **a** winter, **b** pre-monsoon, **c** summer monsoon and **d** post-monsoon season. The first row represents the lower tropospheric (850 hPa) vorticity (shaded; unit 10^{-5} s^{-1}), wind (vector; unit ms^{-1}) and wind speed (contour; unit ms^{-1}). The second row represents the vertical wind shear between lower (850 hPa) and upper (200 hPa) tropospheric levels (shaded; unit ms^{-1}), wind (vector; unit ms^{-1}) and wind speed (contour; unit ms^{-1}) at upper troposphere. The third row represents the middle layer (700–600 hPa) specific humidity (shaded; unit g kg^{-1}) and air temperature (contour; unit °K). The fourth row represents the boundary layer (1000–925 hPa) specific humidity (shaded; unit g kg^{-1}) and tropical cyclone outflow layer (200–150 hPa) temperature (contour unit °K)

for the enhanced potential intensity (fourth row of Fig. 8b). Emanuel (1988) showed that the potential intensity of the TC is proportional to the saturation deficit in the boundary layer. The lesser amount of atmospheric boundary layer humidity enhances the strength of the air-sea enthalpy fluxes because evaporation will be more in a drier atmospheric boundary layer compared to near saturated boundary layer. Hence the higher saturation deficit in the boundary layer of the model favours more number of TC genesis.

During the summer monsoon season, higher TC activity in the model is seen over the northern region of NIO (north BoB and north AS) (Fig. 7c). The decrease in the wind shear and moisture saturation deficit along with the increase in the environmental vorticity are responsible for the enhanced TC activity in the model compared to the observation. The high GPI values over north BoB also postulates excessive formation of weaker cyclonic systems that frequently occur during the summer monsoon season known as monsoon depressions. Anomalous environmental cyclonic vorticity over NIO in the model compared to the observation is due to the weakening of summer monsoon circulation with the southward shift in the core of lower jet stream (Joseph and Raman 1966; Findlater 1969) in the model (first row of Fig. 8c). The weakening of monsoon circulation in the lower (850 hPa) and upper (200 hPa) troposphere is also responsible for the anomalous reduction in the wind shear (first and the second row of Fig. 8c). Even though the simulated air temperature is similar to the observation in the middle tropospheric layer, the higher amount of specific humidity in the model reduces the saturation deficit (third row of Fig. 9c) which is favourable for the genesis/intensification of tropical storms during in the summer monsoon season.

In the post-monsoon season, the model difference in the TCF compared to observation shows a meridional dipole-like structure with enhanced TC activity over southern BoB and suppressed TC activity in the northern BoB (Fig. 7d).

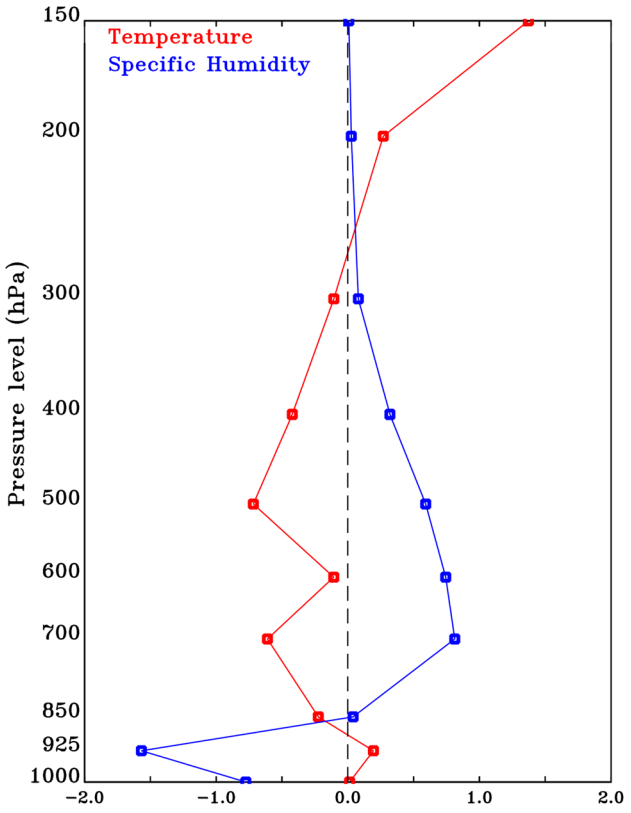

Fig. 9 Annual mean model bias in the vertical profile of air temperature (red; unit °K) and specific humidity (blue; unit g kg^{-1}) averaged over north Indian Ocean (0°–30°N, 50°–100°E) for all periods

This dipole like pattern in the simulated GPI enhanced TC activity over the southern BoB in the model mainly due to the increase in the environmental vorticity and decrease in the wind shear and saturation deficit (Fig. 7d). It may also be noted that suppression of TC activity over northern BoB in the model is mainly from the decrease in the environmental vorticity and the increase in the wind shear over there (Fig. 7d). The strong easterly anomaly in central BoB is responsible for the anomalous cyclonic vorticity in the southern BoB and anticyclonic vorticity in the northern BoB (first row of Fig. 8d). Though the upper-level easterlies are in good agreement with observation, strengthening of unrealistic lower level westerly in the model is responsible for the higher wind shear over northern BoB (first row of Fig. 8d). Reduction in the upper level southeasterly in the southern BoB decreases wind shear in the model (second row of Fig. 8d). Higher specific humidity in the middle layer is responsible for the reduction in the saturation deficit (third row of Fig. 8d). Even though the model has the anomalous increase in the saturation deficit in the boundary layer (fourth row of Fig. 8d), the potential intensity is slightly lower (Fig. 7d). It may be due to the unrealistic high air temperature in the upper tropospheric level in the model (fourth row of Fig. 8d) which reduces the thermodynamic efficiency of the TC intensification (Emanuel 1988) which further reduces the potential intensity of the TC. This reduction in the potential intensity could lessen the strength of the TCs in the model in addition to the model inability which arises from the lower spatial resolution (Davis et al. 2008; Fierro et al. 2009; Manganello et al. 2012).

It is worth to note that the model shows positive bias in the saturation deficit term throughout the seasons (sixth row of Fig. 7). Positive bias in the saturation deficit term indicates the decrease in the saturation deficit in the middle tropospheric layer. In other words, the model requires only less moisture to attain saturation compared to the observation. The decrease in the saturation deficit has a vital role in the higher TC activity during all the season in the model compared to the observation (see Figs. 1 and 3). The difference in the annual average vertical profile of specific humidity and air temperature over NIO shows that model middle tropospheric layers are wetter and colder (Fig. 9) which result in the reduction of saturation deficit in the model. In addition to the factors mentioned above, there exists cold bias in the model for most of the vertical levels except lower layers (1000–925 hPa). Further the combined effect of the decrease in the specific humidity and increase in the temperature in the boundary layer (1000–925 hPa) of the model cause dryness over there (Fig. 9), which is a favourable condition for intensification of the TC activity through the enhanced potential intensity. Hence, the model bias in the thermodynamic parameters such as air temperature and specific humidity are mainly responsible for the unusually higher cyclonic activity in the model in addition to the change in the mean circulation pattern in various seasons.

4 Conclusions and discussion

In this study, the ability of the CORDEX-SA regional models to simulate the climatology, seasonal variation and the intensity of TCs over NIO is evaluated. The outputs obtained from RegCM4 and RCA4 models forced by ERA-Interim reanalysis from 1979 to 2008 with a spatial resolution of 50 km are used for the evaluation of the TC.

- The simulated climatological mean spatial pattern of TGF and TCF by the models are in reasonable agreement with the observation. The RegCM4 model has better skill in producing the mean location of the genesis of TCs and its track compared to the RCA4 model. The overestimation of TC activity in the southern AS in the RCA4 model is the reason for the relatively lesser skill of the model. The anomalous background large scale cyclonic

circulation over southern AS in the RCA4 model may be responsible for the high TC activity over there.

- The models simulate the monthly variation of TGF exhibiting bimodal nature with two peak seasons during pre-monsoon and post-monsoon as in the observation. However, RegCM4 model overestimates the number of TC in all the season with the presence of TCs during the winter season, the season in which very less cyclone activity in the observation. It is mainly due to the overestimated TC genesis near to the equator in the model. Suppressed wind shear, which is favourable for the TC activity in the equatorward of NIO, might be responsible for the high TC activity during the winter season.
- Both the model underestimates the intensity of TC in terms of MVEL and MSLP. However, the simulated relationship between MVEL and MSLP is same as compared to that of observation, albeit higher values in MSLP corresponding MVEL.
- Large-scale environmental factors which are responsible for the genesis of the TC in the RegCM4 model is analyzed using GPI. The model well simulated the differences in the enhanced/suppressed environmental condition during different seasons as in observation, which is responsible for the seasonal variation of TCs.
- The RegCM model overestimates the number of TCs in all the seasons compared to the observation and this due to the enhanced large-scale environmental parameters in the model. The changes in the model circulation modulate the environmental vorticity and wind shear, which makes the environment more conducive for TC genesis. Apart from this, the reduction in the saturation deficit in the middle layer in the model during all the seasons could have an important role in the overestimation of TC genesis. The enhanced specific humidity and decreased air temperature over middle tropospheric level increase (reduce) moisture content (saturation deficit) that could saturate the middle tropospheric levels in a developing cyclonic system promptly, hence favours the genesis/intensification of the TC in the model.

These results suggest that even though regional climate models in the south Asia domain of CORDEX project have the reasonable skill to simulate the mean features of the climate variables, the model simulation shows positive bias in the number of TC in most of the seasons. The difference in the TC activities in the RCMs to the observation in other basins has also reported (Landman et al. 2005; Jin et al. 2013; Diro et al. 2014). The skill of regional RCM to capture the TC activity is sensitive to various parameters such as resolution of the model, convective and surface flux parameterization schemes schemes, flux parameterization, boundary forcing, boundary and size of model domain (Ratnam et al. 2009; Murakami et al. 2013, Diro et al. 2014; Fuentes-Franco et al. 2017; Di Sante et al. 2019). Fuentes-Franco et al. (2017) showed that MIT cumulus parameterization, which is used in this analysis, has a relatively lower skill compared to the Kain–Fritsch scheme in terms of climatological TC activity and intensity of storm in Atlantic and Pacific region. Further, Ratnam et al. (2009) and Di Sante et al. (2019) showed that RegCM4 model with coupled air-sea interaction, which has a better representation of SST-convection feedback, plays an essential role in the interannual and intraseasonal variation in the north Indian Ocean. Hence, it is necessary to analyze the different parameterization schemes (such as cumulus parameterization, microphysics, surface flux parameterization) and associated dynamics to improve the model physics to attain better skill in simulating the TCs over NIO. Therefore, improvement in the model physics will give the reliable future projection of TC activity in the NIO.

Camargo et al. (2007b) showed that the differences in the models to simulate the climatology of TC also arise from the differences in the dynamics of the simulated storms in the model in addition to the differences in the large-scale environment condition. The consistency of climatology of TC with the large-scale environmental variables is better for the model which have a higher spatial resolution (McDonald et al. 2005; Chauvin et al. 2006). Further, previous studies point out that models require high horizontal resolution (at least 10 km) to simulate the TC with reasonable accuracy (Davis et al. 2008; Fierro et al. 2009; Manganello et al. 2012). The increase in the horizontal resolution yields a more realistic simulation of TCs. Hence, in addition to the improvement of model physics that requires the better skill to simulate the large-scale dynamic and thermodynamic variable that responsible for the TC genesis/intensification, the higher resolution of the model also demanded better simulation the TC.

Acknowledgements The IITM-RegCM4 simulations were performed using the IITM Aaditya high power computing resources. The Director, IITM, is gratefully acknowledged for extending full support to carry out this research work. IITM receives full support from the Ministry of Earth Sciences, Government of India. The World Climate Research Programme's Working Group on Regional Climate and the Working Group on Coupled Modelling, the former coordinating body of CORDEX and responsible panel for CMIP5, are sincerely acknowledged. The climate modelling groups (listed in Table 1) are sincerely thanked for producing and making available their model output. The Earth System Grid Federation infrastructure (ESGF; http://esgf.llnl.gov/index.html) is also acknowledged. We would like to acknowledge the two anonymous reviewers, whose comments and suggestions significantly improved the final manuscript.

References

Bechtold P, Bazile E, Guichard F, Mascart P, Richard E (2001) A mass-flux convection scheme for regional and global models. Q J R Meteorol Soc 127:869–886

Bender MA, Knutson TR, Tuleya RE, Sirutis JJ, Vecchi GA, Garner ST, Held IM (2010) Modeled impact of anthropogenic warming on the frequency of intense Atlantic hurricanes. Science 327(5964):454–458

Bengtsson L, Hodges KI, Roeckner E (2006) Storm tracks and climate change. J Clim 19(15):3518–3543

Bengtsson L, Hodges KI, Esch M (2007) Tropical cyclones in a T159 resolution global climate model: comparison with observations and re-analyses. Tellus A 59(4):396–416

Bretherton CS, McCaa J, Grenier H (2004) A new parameterization for shallow cumulus convection and its application to marine subtropical cloud-topped boundary layers. Part I: description and 1d results. Mon Weather Rev 132:864–882

Broccoli AJ, Manabe S (1990) Can existing climate models be used to study anthropogenic changes in tropical cyclone climate? Geophys Res Lett 17:1917–1920. https://doi.org/10.1029/GL017i011p01917

Camargo SJ, Emanuel KA, Sobel AH (2007a) Use of a genesis potential index to diagnose ENSO effects on tropical cyclone genesis. J Clim 20:4819–4834

Camargo SJ, Li H, Sun L (2007b) Feasibility study for downscaling seasonal tropical cyclone activity using the NCEP regional spectral model. Int J Climatol 27:311–325. https://doi.org/10.1002/joc.1400

Camargo SJ, Sobel AH, Barnston AG, Emanuel KA (2007c) Tropical cyclone genesis potential index in climate models. Tellus A 59(4):428–443

Camargo SJ, Wheeler MC, Sobel AH (2009) Diagnosis of the MJO modulation of tropical cyclogenesis using an empirical index. J Atmos Sci 66(10):3061–3074

Cha DH, Jin CS, Lee DK, Kuo YH (2011) Impact of intermittent spectral nudging on regional climate simulation using Weather Research and Forecasting model. J Geophys Res 116:D10103

Chauvin F, Royer JF, Déqué M (2006) Response of hurricane-type vortices to global warming as simulated by ARPEGE-Climat at high resolution. Clim Dyn 27:377–399. https://doi.org/10.1007/s00382-006-0135-7

Choudhary A, Dimri AP, Maharana P (2017) Assessment of CORDEX-SA experiments in representing precipitation climatology of summer monsoon over India. Theor Appl Climatol. https://doi.org/10.1007/s00704-017-2274-7

Christensen JH, Carter TR, Rummukainen M, Amanatidis G (2007) Evaluating the performance and utility of regional climate models: the PRUDENCE project. Clim Change 81:1–6

Davis C, Wang W, Chen SS, Chen Y, Corbosiero K, DeMaria M, Dudhia J, Holland G, Klemp J, Michalakes J, Reeves H, Rotunno R, Snyder C, Xiao Q (2008) Prediction of landfalling hurricanes with the advanced hurricane WRF model. Mon Weather Rev 136:1990–2005

Dee DP, Uppala SM, Simmons AJ, Berrisford P, Poli P, Kobayashi S, Andrae U, Balmaseda MA, Balsamo G, Bauer P, Bechtold P, Beljaars ACM, van de Berg L, Bidlot J, Bormann N, Delsol C, Dragani R, Fuentes M, Geer AJ, Haimberger L, Healy SB, Hersbach H, Hólm EV, Isaksen L, Kållberg P, Köhler M, Matricardi M, McNally AP, Monge-Sanz BM, Morcrette JJ, Park BK, Peubey C, de Rosnay P, Tavolato C, Thépaut JN, Vitart F (2011) The ERA-Interim reanalysis: configuration and performance of the data assimilation system. Q J R Meteorol Soc 137:553–597. https://doi.org/10.1002/qj.828

DeMaria M (1996) The effect of vertical shear on tropical cyclone intensity change. J Atmos Sci 53(14):2076–2088. https://doi.org/10.1175/1520-0469(1996)053%3c2076:teovso%3e2.0.co;2

Di Sante F, Coppola E, Farneti R, Giorgi F (2019) Indian Summer monsoon as simulated by the regional earth system model RegCM-ES: the role of local air–sea interaction. Clim Dyn. https://doi.org/10.1007/s00382-019-04612-8

Diro GT, Giorgi F, Fuentes-Franco R, Walsh KJ, Giuliani G, Coppola E (2014) Tropical cyclones in a regional climate change projection with RegCM4 over the CORDEX Central America domain. Clim Change 125(1):79–94

Emanuel KA (1987) The dependence of hurricane intensity on climate. Nature 326(6112):483–485

Emanuel KA (1988) The maximum intensity of hurricanes. J Atmos Sci 45:1143–1155

Emanuel KA (1999) Thermodynamic control of hurricane intensity. Nature 401:665–669

Emanuel KA (2003) Tropical cyclones. Annu Rev Earth Planet Sci 31:75–104. https://doi.org/10.1146/annurev.earth.31.100901.141259

Emanuel KA (2010) Tropical cyclone activity downscaled from NOAA-CIRES reanalysis, 1908–1958. J Adv Model Earth Syst 2:12. https://doi.org/10.3894/JAMES.2010.2.1

Emanuel KA (2013) Downscaling CMIP5 climate models shows increased tropical cyclone activity over the 21st century. Proc Natl Acad Sci 110(30):12219–12224

Emanuel KA, Nolan DS (2004) Tropical cyclone activity and the global climate system. Preprints, 26th conference on hurricanes and tropical meteorology, Miami, FL, Am Meteorol Soc A, volume 10

Emanuel KA, Živković-Rothman M (1999) Development and evaluation of a convection scheme for use in climate models. J Atmos Sci 56(11):1766–1782

Evan AT, Camargo SJ (2011) A climatology of Arabian Sea cyclonic storms. J Clim 24(1):140–158

Felton C, Subrahmanyam SB, Murty VSN (2013) ENSO-modulated cyclogenesis over the Bay of Bengal. J Clim 26:9806–9818. https://doi.org/10.1175/JCLI-D-13-00134.1

Fierro AO, Rogers RF, Marks FD, Nolan DS (2009) The impact of horizontal grid spacing on the microphysical and kinematic structures of strong tropical cyclones simulated with the WRF-ARW model. Mon Weather Rev 137:3717–3743

Findlater J (1969) A major low-level air current near the indian ocean during the northern summer. Q J R Meteorol Soc 95:362–380

Fu CB, Wang SY, Xiong Z, Gutowski WJ, Lee DK, McGregor JL, Sato Y, Kato H, Kim JW, Suh MS (2005) Regional climate model intercomparison project for Asia. Bull Am Meteorol Soc 86:257–266

Fuentes-Franco R, Giorgi F, Coppola E, Zimmermann K (2017) Sensitivity of tropical cyclones to resolution, convection scheme and ocean flux parameterization over Eastern Tropical Pacific and Tropical North Atlantic Oceans in the RegCM4 model. Clim Dyn 49(1–2):547–561

Giorgi F, Jones C, Asrar GR (2009) Addressing climate information needs at the regional level: the CORDEX framework. WMO Bull 58:175–183

Giorgi F, Coppola E, Solmon F, Mariotti L, Sylla MB, Bi X, Elguindi N, Diro GT, Nair V, Giuliani G, Turuncoglu UU (2012) RegCM4: model description and preliminary tests over multiple CORDEX domains. Clim Res 52:7–29. https://doi.org/10.3354/cr01018

Girishkumar MS, Ravichandran M (2012) The influences of ENSO on tropical cyclone activity in the Bay of Bengal during October–December. J Geophys Res. https://doi.org/10.1029/2011jc007417

Girishkumar MS, Suprit K, Vishnu S, Prakash VT, Ravichandran M (2015) The role of ENSO and MJO on rapid intensification of tropical cyclones in the Bay of Bengal during October–December. Theor Appl Climatol 120(3–4):797–810

Goswami BN, Ajayamohan RS, Xavier PK, Sengupta D (2003) Clustering of synoptic activity by Indian summer monsoon intraseasonal oscillations. Geophys Res Lett 30(8):1431. https://doi.org/10.1029/2002GL016734

Gray WM (1968) Global view of the origin of tropical disturbances and storms. Mon Weather Rev 96:669–700. https://doi.org/10.1175/1520-0493(1968)096%3c0669:GVOTOO%3e2.0.CO;2

Jin CS, Ho CH, Kim JH, Lee DK, Cha DH, Yeh SW (2013) Critical role of northern off-equatorial sea surface temperature forcing associated with Central Pacific El Niño in more frequent tropical cyclone movements toward East Asia. J Clim 26(8):2534–2545

Jin CS, Cha DH, Lee DK, Suh MS, Hong SY, Kang HS, Ho CH (2016) Evaluation of climatological tropical cyclone activity over the western North Pacific in the CORDEX-East Asia multi-RCM simulations. Clim Dyn 47(3–4):765–778

Joseph P, Raman P (1966) Existence of low level westerly jet stream over peninsular india during july. Indian J Meteorol Geophys 17:407–410

Kiehl JT, Hack JJ, Bonan GB, Boville BA, Breigleb BP, Williamson D, Rasch P (1996) Description of the NCAR community climate model (CCM3), Tech. Rep. NCAR/TN-420+STR, National Center for Atmospheric Research

Kim D, Jin CS, Ho CH, Kim JH, Kim J (2014) Climatological features of WRF-simulated tropical cyclones over the western North Pacific. Clim Dyn 44:3223–3235

Knapp KR, Kruk MC, Levinson DH, Diamond HJ, Neumann CJ (2010) The international best track archive for climate stewardship (IBTrACS): unifying tropical cyclone best track data. Bull Am Meteorol Soc 91:363–376. https://doi.org/10.1175/2009BAMS2755.1

Knutson TR, Sirutis JJ, Garner ST, Held IM, Tuleya RE (2007) Simulation of the recent multidecadal increase of Atlantic hurricane activity using an 18-km-grid regional model. Bull Am Meteorol Soc 88:1549–1565

Knutson TR, McBride JL, Chan J, Emanuel K, Holland G, Landsea C, Held I, Kossin JP, Srivastava AK, Sugi M (2010) Tropical cyclones and climate change. Nat Geosci 3(3):157

Krishnamohan KS, Mohankumar K, Joseph PV (2012) The influence of Madden–Julian oscillation in the genesis of North Indian Ocean tropical cyclones. Theor Appl Climatol 109(1–2):271–282. https://doi.org/10.1007/s00704-011-0582-x

Krishnamurti TN, Correa-Torres R, Latif M, Daughenbaugh G (1998) The impact of current and possibly future sea surface temperature anomalies on the frequency of Atlantic hurricanes. Tellus A 50:186–210

Landman WA, Seth A, Camargo SJ (2005) The effect of regional climate model domain choice on the simulation of tropical cyclone—like vortices in the southwestern Indian Ocean. J Clim 18(8):1263–1274

Lee CS, Edson R, Gray WM (1989) Some large-scale characteristics associated with tropical cyclone development in the North Indian Ocean during FGGE. Mon Weather Rev 117(2):407–426

Lenderink G, Holtslag AAM (2004) An updated length-scale formulation for turbulent mixing in clear and cloudy boundary layers. Q J R Meteorol Soc 130:3405–3427

Li Z, Yu W, Li T, Murty VSN, Tangang F (2013) Bimodal character of cyclone climatology in the bay of bengal modulated by monsoon seasonal cycle. J Clim 26:1033–1046

Liebmann B, Hendon HH, Glick JD (1994) The relationship between tropical cyclones of the western Pacific and Indian Oceans and the Madden–Julian oscillation. J Meteorol Soc Jpn 72:401–412

Manganello JV, Hodges KI, Kinter JL, Cash BA, Marx L, Jung T, Achuthavarier D, Adams JM, Altshuler EL, Huang BH, Jin EK, Stan C, Towers P, Wedi N (2012) Tropical cyclone climatology in a 10-km global atmospheric GCM: toward weather-resolving climate modeling. J Clim 25:3867–3893

McDonald RE, Bleaken DG, Cresswell DR, Pope VD, Senior CA (2005) Tropical storms: representation and diagnosis in climate models and the impacts of climate change. Clim Dyn 25:19–36

Murakami H, Sugi M (2010) Effect of model resolution on tropical cyclone climate projections. Sola 6:73–76

Murakami H, Sugi M, Kitoh A (2013) Future changes in tropical cyclone activity in the North Indian Ocean projected by high-resolution MRI-AGCMs. Clim Dyn 40(7–8):1949–1968

Oleson KW, Niu GY, Yang ZL, Lawrence DM, Thornton PE, Lawrence PJ, Stöckli R, Dickinson RE, Bonan GB, Levis S, Dai A (2008) Improvements to the Community Land Model and their impact on the hydrological cycle. J Geophys Res Biogeosci. https://doi.org/10.1029/2007JG000563

Pal JS, Small EE, Eltahir EA (2000) Simulation of regional-scale water and energy budgets: representation of subgrid cloud and precipitation processes within RegCM. J Geophys Res Atmos 105(D24):29579–29594

Praveen V, Sandeep S, Ajayamohan RS (2015) On the relationship between mean monsoon precipitation and low pressure systems in climate model simulations. J Clim 28(13):5305–5324

Räisänen P, Rummukainen M, Räisänen J (2000) Modification of the HIRLAM radiation scheme for use in the Rossby Centre regional atmospheric climate model. Reports meteorology and climatology 49, Department of Meteorology, University of Helsinki, Finland

Rasch PJ, Kristjánsson JE (1998) A comparison of the CCM3 model climate using diagnosed and predicted condensate parameterizations. J Clim 11(7):1587–1614

Ratnam JV, Giorgi F, Kaginalkar A, Cozzini S (2009) Simulation of the Indian monsoon using the RegCM3-ROMS regional coupled model. Clim Dyn 33:119–139

Reynolds RW, Rayner NA, Smith TM, Stokes DC, Wang W (2002) An improved in situ and satellite SST analysis for climate. J Clim 15(13):1609–1625

Samuelsson P, Gollvik S, Ullerstig A (2006) The land-surface scheme of the Rossby Centre regional atmospheric climate model (RCA3). Report in meteorology 122. SMHI, SE-60176 Norrköping, Sweden, p 25

Sanjay J, Krishnan R, Shrestha AB, Rajbhandari R, Ren GY (2017) Downscaled climate change projections for the Hindu Kush Himalayan region using CORDEX South Asia regional climate models. Adv Clim Change Res 8(3):185–198

Singh OP (2008) Indian Ocean dipole mode and tropical cyclone frequency. Curr Sci 94(1):29–31

Singh S, Ghosh S, Sahana AS, Vittal H, Karmakar S (2017) Do dynamic regional models add value to the global model projections of Indian monsoon? Clim Dyn 48(3–4):1375–1397

Strandberg G, Bärring L, Hansson U, Jansson C, Jones C, Kjellström E, Kupiainen M, Nikulin G, Samuelsson P, Ullerstig A (2015) CORDEX scenarios for Europe from the Rossby Centre regional climate model RCA4 SMHI. Retrieved from http://urn.kb.se/resolve?urn=urn:nbn:se:smhi:diva-2839

Sugi M, Noda A, Sato N (2002) Influence of the global warming on tropical cyclone climatology: an experiment with the JMA global model. J Meteorol Soc Jpn 80:249–272

Taylor KE, Stouffer RJ, Meehl GA (2012) An overview of CMIP5 and the experiment design. Bull Am Meteorol Soc 93(4):485–498

Vishnu S, Francis PA, Shenoi SSC, Ramakrishna SSVS (2016) On the decreasing trend of the number of monsoon depressions in the Bay of Bengal. Environ Res Lett 11(1):014011

Vitart F, Anderson JL, Stern WF (1997) Simulation of interannual variability of tropical storm frequency in an ensemble of GCM integrations. J Clim 10(4):745–760

Walsh KJE, Nguyen KC, McGregor JL (2004) Fine-resolution regional climate model simulations of the impact of climate change on tropical cyclones near Australia. Clim Dyn 22:47–56

Walsh KJ, Fiorino M, Landsea CW, McInnes KL (2007) Objectively determined resolution-dependent threshold criteria for the detection of tropical cyclones in climate models and reanalyses. J Clim 20(10):2307–2314

Yanase W, Satoh M, Taniguchi H, Fujinami H (2012) Seasonal and intraseasonal modulation of tropical cyclogenesis environment over the Bay of Bengal during the extended summer monsoon. J Clim 25(8):2914–2930

Zeng X, Zhao M, Dickinson RE (1998) Intercomparison of bulk aerodynamic algorithms for the computation of sea surface fluxes using TOGA COARE and TAO data. J Clim 11(10):2628–2644